Electronic Supplementary Material (ESI) for Nanoscale.

Supporting Information

Eliminating Nonspecific Binding Sites for Highly Reliable Immunoassay via Super-resolution Multicolor Fluorescence Colocalization

Shenfei Zong[#], Yun Liu[#], Kuo Yang, Zhaoyan Yang, Zhuyuan Wang, Yiping Cui**

[#] These authors contributed equally to this work
Advanced Photonics Center, Southeast University, Nanjing 210096, China
E-mail: wangzy@seu.edu.cn, cyp@seu.edu.cn

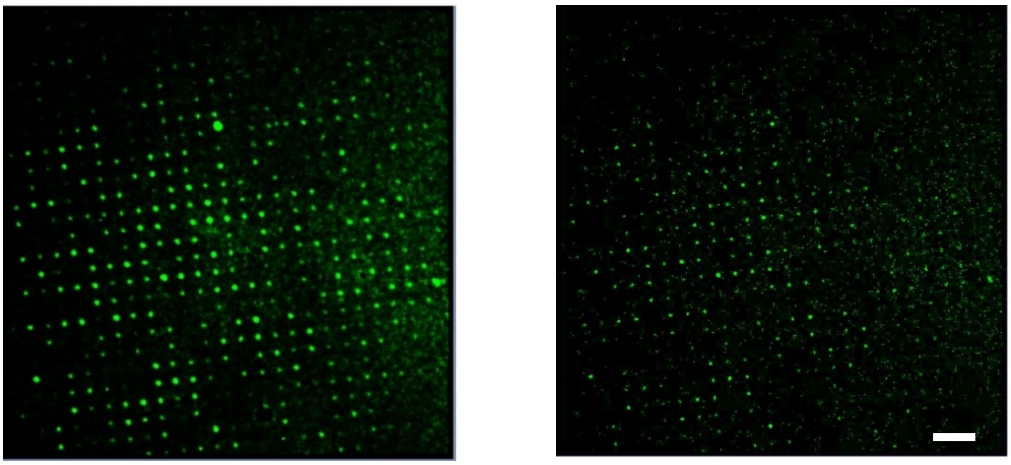

Figure S1. The wide field fluorescence (left) and SMLM (right) images of a gold nanopillar array modified with the capture probes (FAM-HER2-SH). Scale bar: 5 μm. The fluorescence of FAM was collected for imaging.

Detailed preparation process of the imaging chamber

First, the cover glass washed with piranha solution and the edges of the prepared quartz plate to be observed are bonded with waterproof double-sided tape. The thickness of the waterproof double-sided adhesive is 50 microns. Next, imaging buffer was added to the chamber. Then nail polish was used to seal the chamber to prevent the imaging buffer from volatilizing during the experiment. After the nail polish has solidified, fluorescence imaging can be performed. Because the coverslip is relatively brittle, it is easy to break during the imaging process. Therefore, we strengthened the samples using PDMS and slides. The PDMS chip is mixed by 184 silicone rubber and the corresponding curing agent with a volume ratio of 10:1, and placed in a vacuum dish for 30 minutes to remove air bubbles in the solution. After 30 minutes, the mixture was poured into a mold, placed in an oven at 80°C and cured for 45 minutes. The chamber is shown in Figure S2. Figure S2a is a front view of the chamber. Figure S2b is a plan view.

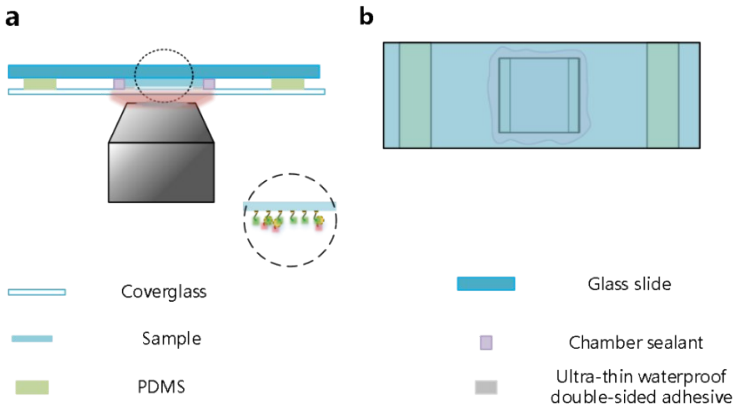

Figure S2. Schematic diagram of the observation chamber.

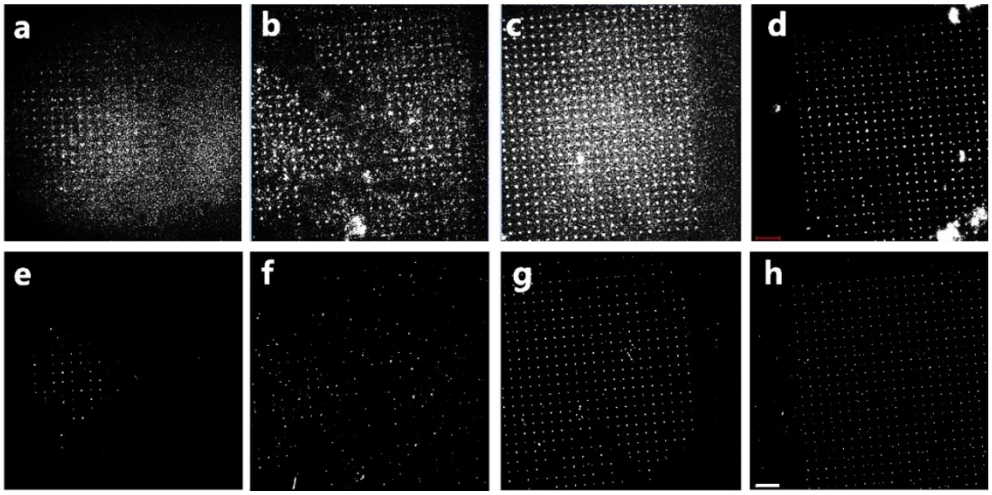

Figure S3. Wide-field images (a-d) and the corresponding SMLM images (e-h) of the arrays modified with different concentrations of the capture probes. The concentrations of the capture probes are 1 μM (a, e), 0.1 μM (b, f), 0.01 μM (c, g) and 1 nM (d, h), respectively. Scale bar: 5 μm.

The necessity of using SMLM in SR-MFC

The reasons why we can ignore the localization precisions of the capture probes and immunoprobes, and why do we have to utilize SMLM in SR-MFC was explained as follows. For a certain round of localization by one frame of WF image, we denote the positions (in the *xy* plane) of the centroids of capture probes and immunoprobes as follows.

Capture probes: $(x_1 + \delta_{x1}, y_1 + \delta_{y1})$,

Immunoprobes: $(x_2 + \delta_{x2}, y_2 + \delta_{y2})$,

where x_1, y_1 and x_2, y_2 represent the accurate coordinates of the centroids of the probes, δ_{x1}, δ_{y1} and δ_{x2}, δ_{y2} represent the localization errors in the *xy* directions of the two probes, respectively. During each round of localization, standard Gaussing fitting was used to determine the positions of the centroids. Considering the symmetry of Gaussing fitting in the *xy* directions, $\delta_{x1}=\delta_{y1}$ and $\delta_{x2}=\delta_{y2}$. By taking thousands of images and repetitively

perform localization using SMLM, we can obtain the averaged positions of the centroids of capture probes and immunoprobes, which can be expressed as follows:

Capture probes: $(x_1 + \bar{\delta}_{x1}, y_1 + \bar{\delta}_{y1})$,

Immunoprobes: $(x_2 + \bar{\delta}_{x2}, y_2 + \bar{\delta}_{y2})$,

where $\bar{\delta}_{x1}, \bar{\delta}_{y1}, \bar{\delta}_{x2}, \bar{\delta}_{y2}$ represent the averaged localization errors.

The distance d between the two centroids is thus

$$d = \sqrt{(x_1 - x_2 + \bar{\delta}_{x1} - \bar{\delta}_{x2})^2 + (y_1 - y_2 + \bar{\delta}_{y1} - \bar{\delta}_{y2})^2}.$$

Statistically, when the localization rounds become large (thousands of times as in SMLM), the averaged localization errors will tend to the localization precisions of the fluorophores. In our experiment, we utilized FAM and Cy5 as the fluorescent tags of the capture probes and immunoprobes, because the localization precisions of them are comparable to each other (Figure S6). Consequently, when the localization rounds became large, $\bar{\delta}_{x1}, \bar{\delta}_{y1}, \bar{\delta}_{x2}, \bar{\delta}_{y2}$ would gradually get equivalent to each other and the distance d between the two centroids becomes

$$d = \sqrt{(x_1 - x_2)^2 + (y_1 - y_2)^2}$$

This means by using SMLM, the localization precision is no longer a problem and we can obtain the exact distance between the capture probes and immunoprobes. The only requirement is that the localization precisions of the fluorophores on capture probes and immunoprobes should be equal.

When the errors of a single localization is small enough (e.g. several nanometers when detecting small targets such as proteins), we can simplify the experimental setup to perform only common WF imaging, which can eliminate the use of specialized blinking labels or imaging buffers as suggested by the reviewer. Localization once with such a high precision could be achieved with the single molecule fluorescence technique.

However, there are multiple capture probes on a nanopillar and more than one immunoprobes could bind to this site, localization the centroids of multiple emitters for once may induce a relatively large error. The data in Figure 4 and Figure S10 showed that localization with a single WF image is not as good as SMLM. For example, the LOD of single WF image based colocalization is about an order higher than that of SMLM (Figure S10). Considering all above, the SMLM based localization is necessary in our experiment, which can improve the accuracy of the obtained distance d by many rounds of localization.

Although SMLM imaging performed better than the WF imaging, under certain circumstances, WF imaging is sufficient enough for multicolor fluorescence colocalization based elimination of the nonspecific reaction sites. For example, if we are not pursuing a low LOD, WF imaging should work because it can also produce a concentration dependent response (Figure S10).This would greatly simplify the detection scheme and reduce cost (because the SMLM imaging system and special buffers are no longer needed).

The significance of the arrayed gold nanopillars in SR-MFC

There is a possibility that the immunoprobes would bind directly to the capture probes, their fluorescence signals surely would overlap well with each other in the SMLM images, and it is impossible for us to discriminate these nonspecific adsorption sites from the specifically interaction ones using the current two-color SMLM imaging based colocalization. In a common immunofluorescence assay, the capture probes are modified homogeneously on a flat substrate (e.g. glass slide or polystyrene plate). If the immunoprobes adsorb onto the substrate, they will always fall onto the capture probes, resulting in nonspecific binding that can not be discriminated by SR-MFC. To solve this problem, we utilized arrayed gold nanopillars as the substrate for immobilizing the

capture probes because they provided limited interaction area of the immunoprobes and can greatly reduce the possibility of direct adsorption between the immunoprobes and capture probes.

In the current SR-MFC assay, to simplify the procedures, we assumed that direct interaction between the immunoprobes and capture probes was a rare event. To support such an assumption, the possibility of direct adsorption between the two kinds of probes were analyzed using the SMLM images of the blank control. Figure S4 shows SMLM imaging results of the blank control. The yellow circles pointed out the nanopillars where the fluorescence of immunoprobes and capture probes overlapped, which should be nonspecific adsorption sites where the two kinds of probes adsorbed directly. By simple calculation, we found that the nanopillars adsorbed directly with immunoprobes constituted only about 6.6% of all the nanopillars, which was a quite small fraction. So the assumption should hold that direct adsorption between the immunoprobes and the capture probes was hard to happen in our situation.

In addition to the directly adsorbed nonspecific sites (the yellow circles), there were still a relatively large fraction of the immunoprobes that were adsorbed on the quartz plate (the red circles). Although the current SR-MFC cannot exclude the yellow circled sites, it can totally exclude the red circled ones. Statistically, since the direct adsorption between the immunoprobes and capture probes can be considered as a rare event and the other nonspecific interaction sites (red circles) can be excluded, the overall goal of eliminating nonspecific interaction sites and improving the accuracy of immunoassays still can be realized by the SR-MFC method.

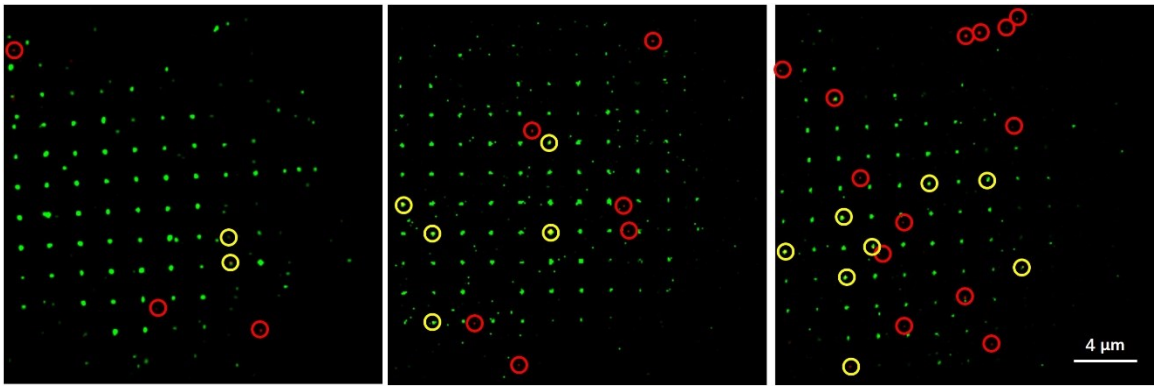

Figure S4. Examples of SMLM imaging results of the nanopillar arrays of the blank control. Merged images of the capture probes (green) and immunoprobes (red) are shown. The yellow circles pointed out the nanopillars where the immunoprobes and capture probes interacted directly. The red circles indicated immunoprobes adsorbed on the quartz plate.

Estimating the sizes of capure probe and immunoprobe

According to Equation (1), d is caluclated by adding the sizes of the analyte, capture probe and immunoprobe. The size of the analytes (exosomes) were obtaind from TEM. The sizes of capture probe and immunoprobe were estimated as follows. The structure of the HER2 aptamer is acquired from previously published literature (*Analyst*, 2015, 140, 243–249). Figure S5 shows the structure of capture probe that we utilized. The fluorophores are linked to the sugar ring or phosphate backbone of the DNA strands, so they will not influence the total length of the aptamer and we omitted them (FAM, Cy5) while estimating the sizes of capture probe and immunoprobe.

The size of a single base is 0.33 nm or that of ten bases is 3 nm, the length of C-C bond is 0.154 nm while that of C-S bond is 0.181 nm (*Journal of the Chemical Society*, Perkin Transactions 2, 1987, S1-S19). Thus, we get the following equations:

$$\pi L_1 = 7 \times 0.33 \text{ nm}$$

$$L_2 = 5 \times 0.33 \text{ nm}$$

$$\pi L_3 = 31 \times 0.33 \text{ nm}$$

$$L_4 = 3 \text{ nm}$$

L_5=6×0.154+0.181 nm

Hence:

The size of capture probe is $S_c=L_1+L_2+L_3+L_4+L_5 \approx 9.71$ nm

The size of immunoprobe is $S_p= L_1+L_2+L_3 \approx 5.6$ nm

The size of the exosomes obtained from TEM image is 25.52 ~ 158.06 nm. Therefore, the maximum d in Equation (1) should be 158.06 nm+9.71 nm+5.6 nm=173.37 nm.

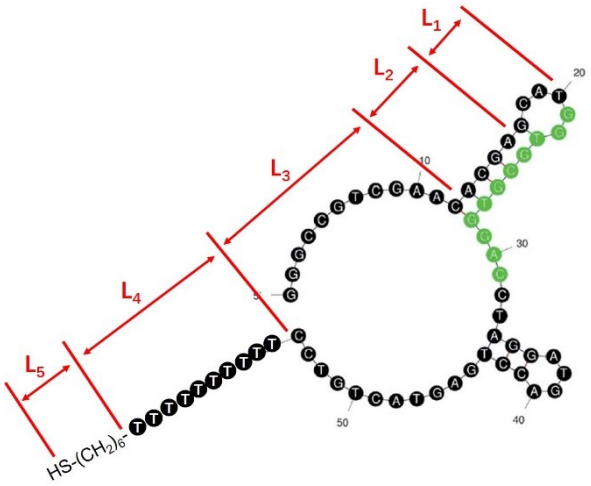

Figure S5. The structure of the capture probe.

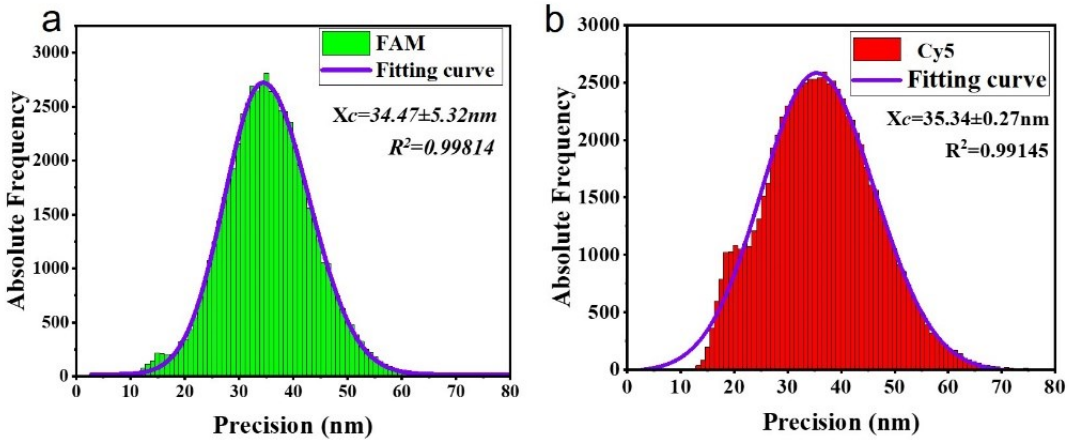

Figure S6. Localization precisions of the FAM channel and Cy5 channel.

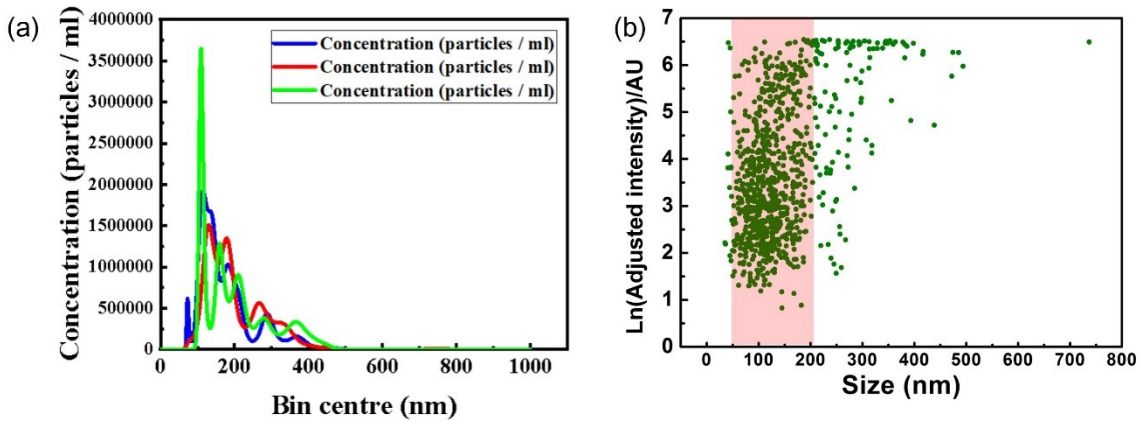

Figure S7. (a) Exosome concentrations obtained by NTA. (b) Hydrodynamic diameter of the exosomes obtained by NTA.

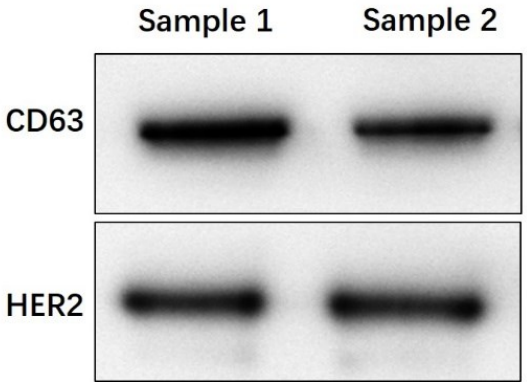

Figure S8. Western blot results of the exosomes. WB was performed by Nanjing KeyGen Biotech. Sample 1 refers to exosomes collected by KeyGen Biotech from the culture media of SKBR3 cells that we provided. Sample 2 refers to exosomes collected by us from the culture media of SKBR3 cells.

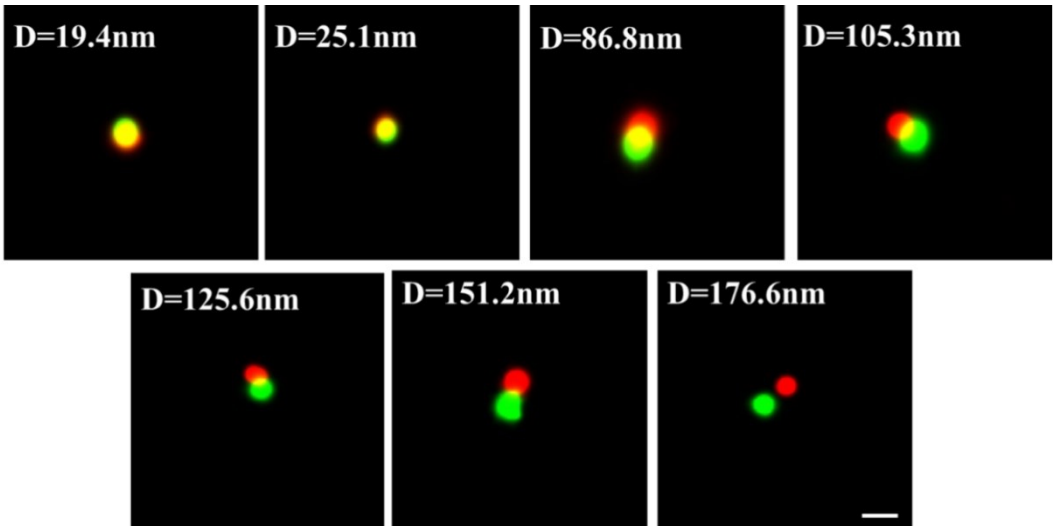

Figure S9. SMLM images of various pairs of capture probes and immunoprobes on different reaction sites with different distance d. Scale bar:200nm.

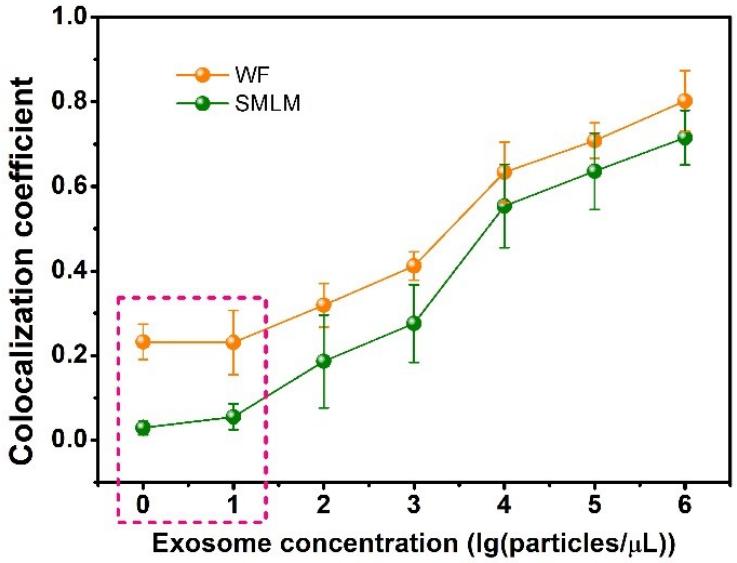

Figure S10. Colocalization coefficients obtained from WF and SMLM images of different concentrations of exosomes.

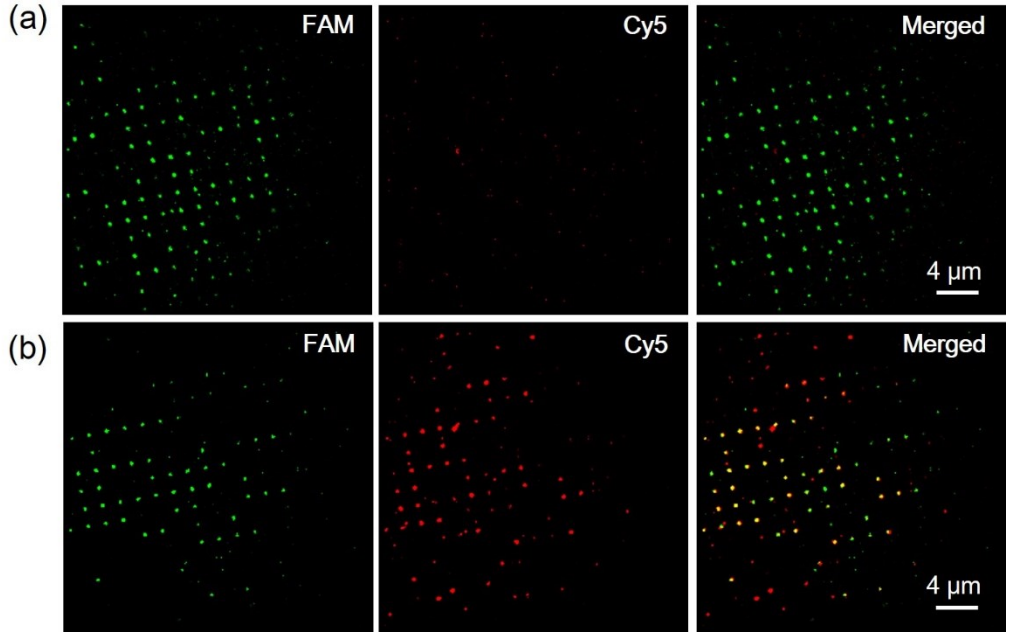

Figure S11. SMLM images of the capture probes (FAM), immunoprobes (Cy5) and their merged images. (a) Healthy human serum. (b) Breast cancer patient's serum. Each SMLM image was reconstructed from 5000 frames of the original wide-field images.

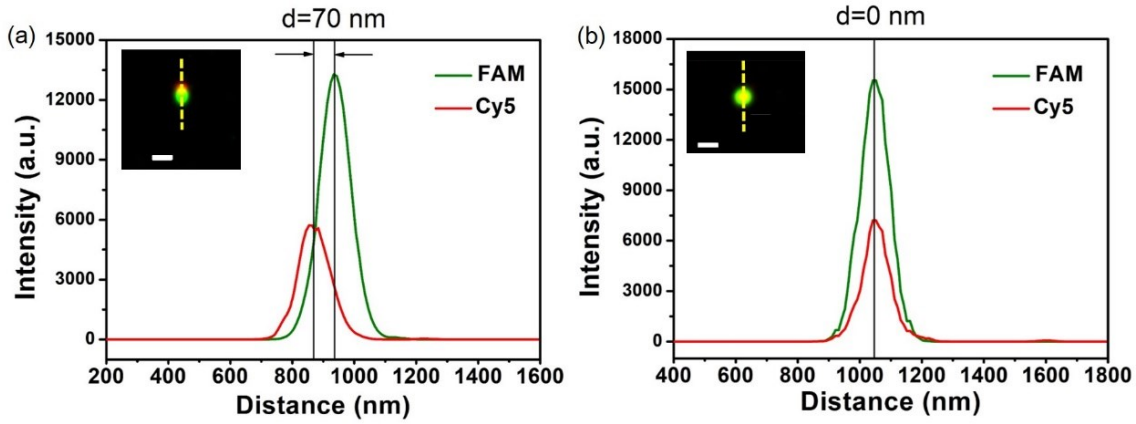

Figure S12. SR-MFC assay results of HER2 protein detection. (a) Nonspecific reaction site, (b) specific reaction site. The insets are merged SMLM images of the FAM (green) and Cy5 (red) channels. The intensity profiles along the dashed lines are presented, respectively. Scale bar: 200 nm.